THE ASSEMBLY OF MILKY WAY-LIKE GALAXIES SINCE Z ∼ 2.5

PIETER G. VAN DOKKUM[1], JOEL LEJA[1], ERICA JUNE NELSON[1], SHANNON PATEL[2], ROSALIND E. SKELTON[1], IVELINA MOMCHEVA[1], GABRIEL BRAMMER[3], KATHERINE E. WHITAKER[4], BRITT LUNDGREN[5], MATTIA FUMAGALLI[2], CHARLIE CONROY[6], NATASCHA FÖRSTER SCHREIBER[7], MARIJN FRANX[2], MARISKA KRIEK[8], IVO LABBÉ[2], DANILO MARCHESINI[9], HANS-WALTER RIX[10], ARJEN VAN DER WEL[10], STIJN WUYTS[7]
Submitted to ApJ Letters

ABSTRACT

Galaxies with the mass of the Milky Way dominate the stellar mass density of the Universe but it is uncertain how and when they were assembled. Here we study progenitors of these galaxies out to $z \sim 2.5$, using data from the 3D-HST and CANDELS Treasury surveys. We find that galaxies with present-day stellar masses of $\log(M) \approx 10.7$ built $\sim 90\%$ of their stellar mass since $z \sim 2.5$, with most of the star formation occurring before $z \sim 1$. In marked contrast to the assembly history of massive elliptical galaxies, the centers and outer parts of the galaxies built up at roughly the same rate between $z \sim 2.5$ and $z \sim 1$. We therefore conclude that a "standard" model for the formation of spiral galaxies, with the bulge assembling first and the disk building around it, is probably not correct. Instead, bulges (and black holes) likely formed in lockstep with disks, through bar instabilities, clump migration, or other processes. We find that after $z \sim 1$ the growth in the central regions gradually stopped and the disk continued to build, consistent with recent studies of the gas distributions in $z \sim 1$ galaxies and the properties of many spiral galaxies today.

Subject headings: cosmology: observations — galaxies: evolution — Galaxy: structure — Galaxy: formation

1. INTRODUCTION

The Milky Way is a very typical galaxy, in the sense that a randomly chosen star in the Universe is most often found in a bulge – disk system of similar mass. Despite their ubiquity, and our exquisite knowledge of one example of their class, the assembly history of large spiral galaxies is still very uncertain (see Rix & Bovy 2013, and references therein). Disks are thought to form through gas accretion, with the structure of the disks largely determined by the angular momentum of the dark matter halo (Mo, Mao, & White 1998). In many models for galaxy formation bulges arise from the merger of two disks, after which a new disk can form (e.g., Kauffmann, White, & Guiderdoni 1993). In the context of these models the Milky Way bulge formed before the disk (see also, e.g., Zoccali et al. 2006; Okamoto 2013). This "inside-out" scenario is qualitatively similar to the assembly history of massive ellipticals, which formed a dense core at high redshift and then built up their outer parts (e.g., van Dokkum et al. 2010; Hilz, Naab, & Ostriker 2013).

However, recent theoretical and observational studies have challenged this picture. In cosmological simulations of gas accretion the structure of the forming galaxy not only depends on the properties of the dark matter but also on the details of the feedback mechanism (e.g., Agertz, Teyssier, & Moore 2011; Brooks et al. 2011) and on the accretion mode (e.g., Sales et al. 2012). Furthermore, major mergers are probably too rare to form many bulges (e.g., Kitzbichler & White 2008), and several studies have suggested alternative ways to build up central mass concentrations. In particular, bulges may be built by "direct injection" of gas in cold streams (e.g., Sales et al. 2012) and/or by the migration of star forming clumps in unstable disks (Elmegreen, Bournaud, & Elmegreen 2008; Dekel et al. 2009; Krumholz & Dekel 2010). Such clumpy, unstable, rapidly star-forming disks have been shown to exist at high redshift (e.g., Genzel et al. 2008; Förster Schreiber et al. 2011).

In this paper (and in Patel et al. 2013b, which uses a complementary approach) we provide new constraints on the assembly of disks and bulges by studying plausible progenitors of Milky Way-mass galaxies in the 3D-HST survey (Brammer et al. 2012). The immediate goals are to determine the typical star formation histories of these galaxies and to assess when their major structural components were assembled. The data also provide key constraints on the ingredients in recent hydrodynamical models: these models now succeed in reproducing many of the properties of the present-day Milky Way (Brooks et al. 2011; Guedes et al. 2011) and to improve them further we need to test their predictions at earlier times. A Kroupa (2001) IMF is assumed throughout the paper.

2. MASS EVOLUTION

Following previous studies (e.g., van Dokkum et al. 2010; Papovich et al. 2011; Patel et al. 2013a; Leja, van Dokkum, & Franx 2013) we link progenitor and descendant galaxies by requiring that they have the same (cumulative) co-moving number density. Effectively, galaxies are ranked according to their stellar mass and we study galaxies at high redshift that have the same rank order as the Milky Way does at $z = 0$. The implicit assumption is that rank order is conserved through

[1] Department of Astronomy, Yale University, New Haven, CT 06511, USA

[2] Leiden Observatory, Leiden University, Leiden, The Netherlands

[3] European Southern Observatory, Alonson de Córdova 3107, Casilla 19001, Vitacura, Santiago, Chile

[4] Astrophysics Science Division, Goddard Space Center, Greenbelt, MD 20771, USA

[5] Department of Astronomy, University of Wisconsin-Madison, Madison, WI 53706, USA

[6] Department of Astronomy & Astrophysics, University of California, Santa Cruz, CA, USA

[7] Max-Planck-Institut für extraterrestrische Physik, Giessenbachstrasse, D-85748 Garching, Germany

[8] Department of Astronomy, University of California, Berkeley, CA 94720, USA

[9] Department of Physics and Astronomy, Tufts University, Medford, MA 02155, USA

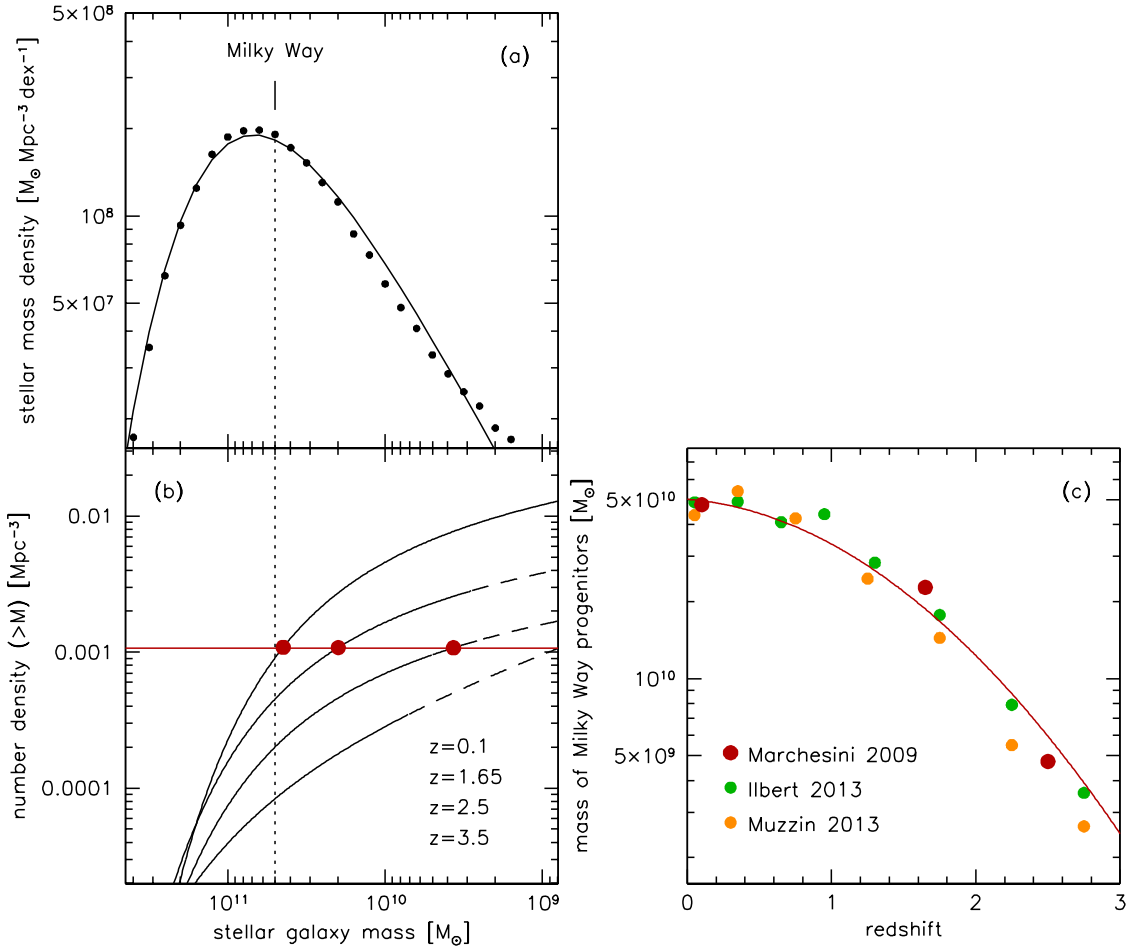[10] Max Planck Institute for Astronomy (MPIA), Königstuhl 17, D-69117, Heidelberg, Germany

Figure 1. *(a)* Stellar mass density of the Universe as a function of galaxy mass, as determined from the SDSS-GALEX $z = 0.1$ mass function of Moustakas et al. (2013). *(b)* Evolution of the cumulative galaxy mass function from $z = 0.1$ to $z = 3.5$ (SDSS-GALEX and Marchesini et al. 2009). The horizontal line indicates a constant cumulative co-moving number density of 1.1×10^{-3} Mpc^{-3}. *(c)* Mass evolution at a constant number density of 1.1×10^{-3} Mpc^{-3}.

cosmic time, or that processes that break the rank order do not have a strong effect on the average measured properties. As shown in Leja et al. (2013) the method recovers the true mass evolution of galaxies remarkably well in simulations that include merging, quenching, and scatter in the growth rates of galaxies.

The present-day stellar mass of the Milky Way is approximately $5 \times 10^{10} M_\odot$ (Flynn et al. 2006; McMillan 2011). Using the SDSS-GALEX stellar galaxy mass function of Moustakas et al. (2013) we find that galaxies with masses $> 5 \times 10^{10} M_\odot$ have a number density of 1.1×10^{-3} Mpc^{-3}. We then trace the progenitors of these galaxies by identifying, at each redshift, the mass for which the cumulative number density is 1.1×10^{-3} Mpc^{-3} (see Fig. 1b). We used the Marchesini et al. (2009) mass functions as they are complete in the relevant mass and redshift range; we verified that the results are similar when other mass functions are used (Ilbert et al. 2013; Muzzin et al. 2013).

The stellar mass evolution for galaxies with the rank order of the Milky Way is shown in Fig. 1c. The evolution is rapid from $z \sim 2.5$ to $z \sim 1$ and relatively slow afterward. We therefore approximate the evolution with a quadratic function of the form

$$\log(M_{\rm MW}) = 10.7 - 0.045z - 0.13z^2. \qquad (1)$$

Based on the variation between mass functions of different authors, and the results of Leja et al. (2013), we estimate that the uncertainty in the evolution out to $z \sim 2.5$ is approximately 0.2 dex.[11] More than half of the present-day mass was assembled in the 3 Gyr period between $z = 2.5$ and $z = 1$, and as we show later the mass growth is likely dominated by star formation at all redshifts. The mass evolution is significantly faster than that of more massive galaxies (van Dokkum et al. 2010; Patel et al. 2013a), consistent with recent results of Muzzin et al. (2013).

3. MILKY WAY PROGENITORS FROM $Z = 0$ TO $Z = 2.5$

3.1. *Rest-frame Images*

Having determined the stellar mass evolution with redshift, we can now select galaxies in mass bins centered on this evolving mass and study how their properties changed. We selected galaxies in GOODS-North and GOODS-South as these fields have multi-band ACS and WFC3 imaging (from the GOODS and CANDELS surveys respectively; Giavalisco et al. 2004; Grogin et al. 2011; Koekemoer et al. 2011), as well as WFC3 G141 grism spectra from the 3D-HST program

[11] We verified that changing the evolution does not affect the key results of this paper.
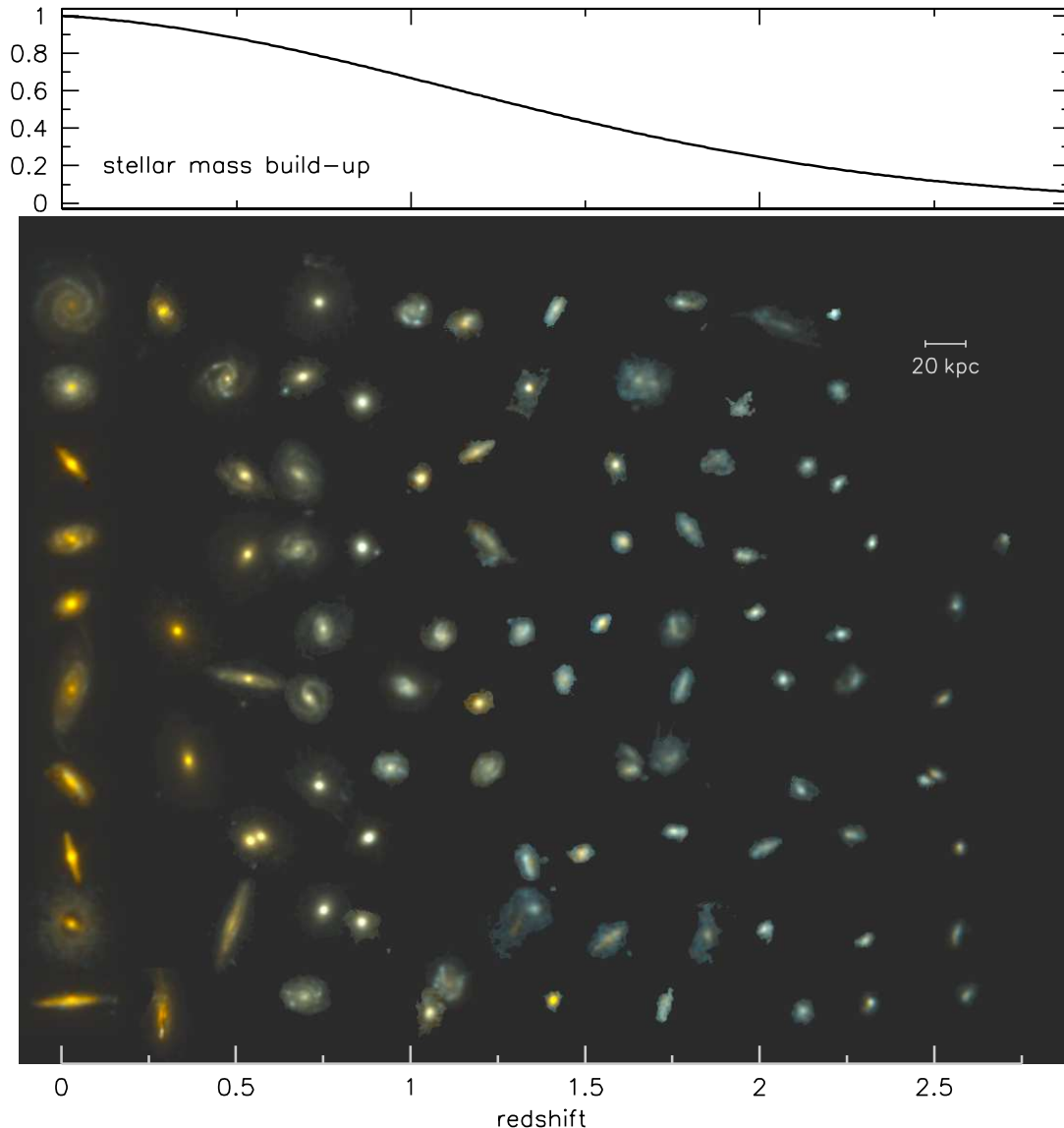
Figure 2. Examples of galaxies with the number density of the Milky Way at $0 < z < 2.75$. Galaxies at $z \approx 0.015$ are from the SDSS; galaxies at higher redshift are from the 3D-HST and CANDELS surveys. The color images were created from data in the same rest-frame bands (u and g) at all redshifts and have a common physical scale. Their intensities are scaled so they are proportional to mass, indicated in the top panel. Galaxies at high redshift have relatively low surface densities; their centers and outer parts seem to build up at the same time, at least until $z \sim 1$.

(Brammer et al. 2012). Redshifts, stellar masses, and star formation rates were determined from deep photometric catalogs in these fields, combined with the grism spectra (see Brammer et al. 2012 and references therein, and R. Skelton et al., in preparation). The 3D-HST v2.1 catalos are $\approx 100\%$ complete in the relevant mass and redshift range, but we note that we rely almost exclusively on photometric redshifts (rather than grism redshifts) at $z \gtrsim 1.3$.

There are 361 galaxies at $0.25 < z < 2.75$ in the catalogs whose mass is within ± 0.1 dex of $M_{\rm MW}(z)$. Images of a random subset of 90 are shown in Fig. 2. The images have the same physical scale and represent the same rest-frame filters (u and g). Their brightness is scaled in such a way that their total ($u + g$) flux is proportional to $M_{\rm MW}(z)$. The rest-frame u and g images were created by interpolating the two ACS and/or WFC3 images (smoothed to the H_{160} resolution) whose central wavelengths are closest to the redshifted u and g filters.

Also shown are nearby galaxies from the Sloan Digital Sky Survey (SDSS). We selected 40 galaxies with $0.013 < z < 0.017$ and $10.62 < \log M < 10.78$ from the DR7 MPA-JHU catalogs[12] (Brinchmann et al. 2004), and degraded their u and g images to the same spatial resolution as the high redshift galaxies. A random subset of 10 are shown in Fig. 2.

It is clear from Fig. 2 that present-day galaxies with the mass of the Milky Way have changed over cosmic time. The most obvious change is that galaxies became redder with time, particularly after $z \sim 1$, indicative of a decrease in the specific star formation rate. The galaxies also appear brighter at lower redshift in Fig. 2, reflecting the mass evolution of Eq. 1. A striking aspect of this change in brightness, and the central

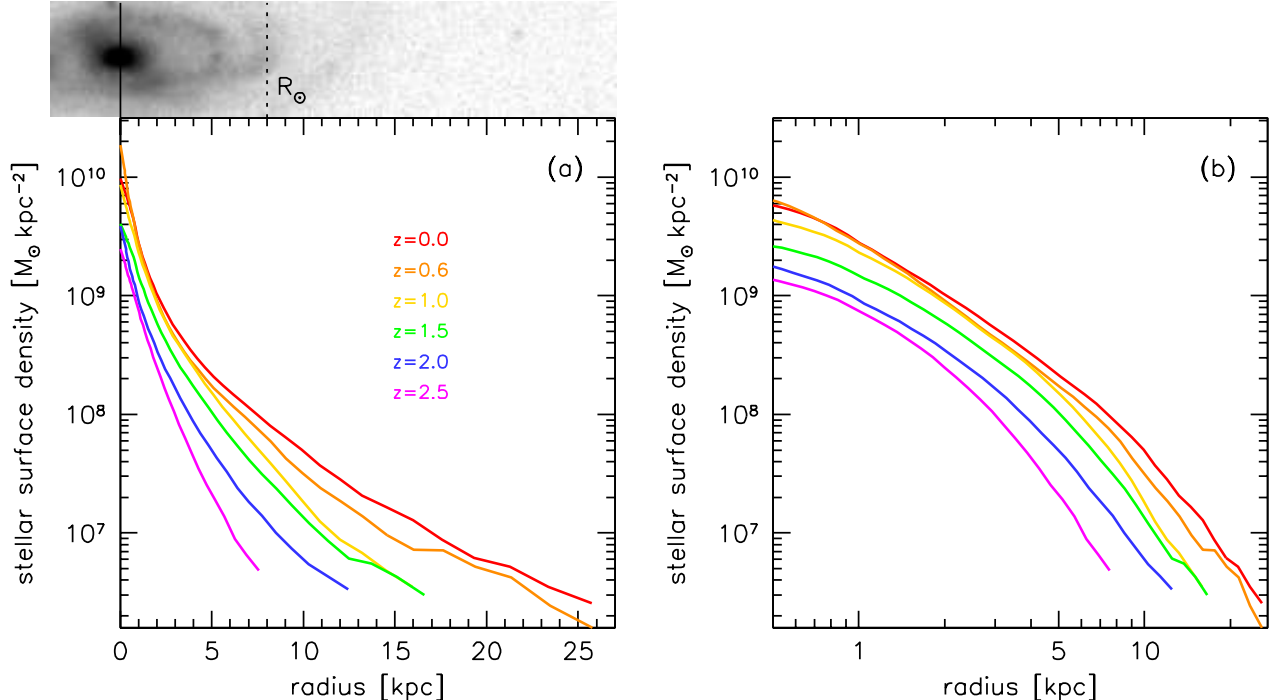**Figure 3.** Surface density profiles from $z = 2.5$ to $z = 0$, as measured from averaged, PSF-corrected rest-frame g band images in each redshift bin. The horizontal axis is linear in *(a)* and logarithmic in *(b)*. The galaxy image is randomly chosen from our SDSS sample to illustrate the radial extent of the profiles. The main evolution is in normalization, which is determined by $M_{MW}(z)$ (Eq. 1). The profile *shapes* are very similar from $z \sim 2.5$ to $z \sim 1$, which implies that the galaxies are building up their mass at all radii. After $z \sim 1$ the central regions stop growing but the disk continues to build.

result of this paper, is that the bulges appear to change just as much as the disks, particularly at $z > 1$. We do *not* see high density "naked bulges" at $z \sim 2$ around which disks gradually assembled. Instead, the central densities at $z \sim 2$ were much lower than the central densities at $z \sim 0$. We quantify this result in the remainder of the paper.

3.2. *Evolution of Surface Density Profiles*

We first analyze the surface density profiles of the galaxies to study their mass growth as a function of radial distance from their centers. Following van Dokkum et al. (2010) we measured the profiles from stacked images to increase the signal-to-noise ratio. The galaxies were grouped in six bins with mean redshifts 0.015, 0.60, 1.0, 1.5, 2.0, and 2.4. Each bin contains at least 40 galaxies. The rest-frame u and g band images in each bin were normalized and stacked, aggressively masking all neighboring objects.

The image stacks were corrected for the effects of the point spread function (PSF) following the method outlined in Szomoru et al. (2010). First, a two-dimensional Sersic (1968) model, convolved with the PSF, was fit to the stacks using the GALFIT code (Peng et al. 2010). Then the residuals of this fit were added to the *un*convolved Sersic model. As shown in Szomoru et al. (2010) this method reconstructs the true flux distribution with high fidelity, even for galaxies that are poorly fit by Sersic profiles. The resulting radial surface density profiles are shown in Fig. 3. The profiles are derived from the rest-frame g band images and scaled such that the total mass within a diameter of 50 kpc is equal to $M_{MW}(z)$. We note here that the $u - g$ color gradients of the stacks are small (≈ 0.1 dex^{-1}) at all redshifts, consistent with other studies (e.g., Szomoru et al. 2013).

There is strong evolution in the overall normalization of the

profiles from $z = 2.5$ to $z = 1$ and less evolution thereafter, reflecting the mass evolution of Eq. 1. The evolution from $z = 2.5$ to $z = 1$ is strikingly uniform: the profiles are roughly parallel to one another in Fig. 3b, and rather than mostly assembling inside-out the galaxies increase their mass at all radii at approximately the same rate. This is in marked contrast to more massive galaxies, which form their cores early and exclusively build up their outer parts over this redshift range (see Fig. 6 in van Dokkum et al. 2010 and Fig. 6 in Patel et al. 2013a). After $z \sim 1$ the evolution in the central parts slows down but the outer parts continue to build up, consistent with the visual impression that around this time the classical "quiescent bulge and star forming disk" structure of spiral galaxies was established (see Fig. 2).

3.3. *Mass Growth at Different Radii*

We explicitly show the mass growth at different radii in Fig. 4a. From $z \sim 2.5$ to $z \sim 1$ the mass within $r = 2$ kpc and the mass outside of 2 kpc increase at approximately the same rate, mirroring the increase in the total mass over this time interval. Again, this trend is qualitatively different from that seen in more massive galaxies: after $z \sim 2$ the mass within 2 kpc is constant to within 0.1 dex for galaxies with $\log(M/M_\odot)(z = 0) = 11.2$ (see Fig. 7 of Patel et al. 2013a). After $z \sim 1$ the trend is similar to that for more massive galaxies: the central mass is approximately constant, whereas the mass at large radii continues to grow.

In Fig. 4b we express the growth in mass as an (implied) star formation rate. The star formation rate was calculated directly from Eq. 1, with a $\times 1.35$ upwards correction to account for mass loss in winds.[13] The implied star formation rate is ap-

---

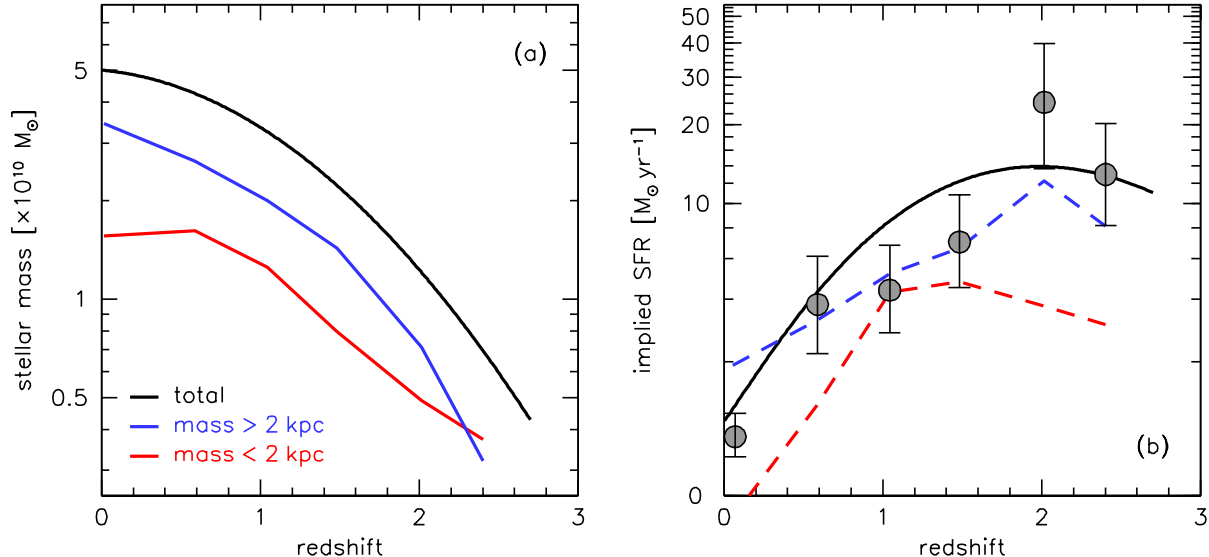[13] This factor is the mass loss after 2 Gyr for a Kroupa (2001) IMF.

Figure 4. *(a)* Comparison of the mass growth in the central regions to the growth at larger radii. The galaxies grow at all radii until $z \sim 1$, after which the mass inside $r = 2$ kpc remains roughly constant. *(b)* Implied evolution of the star formation rate. Data points are the mean measured star formation rates of the galaxies in each redshift bin, from the 3D-HST v2.1 catalogs (Skelton et al., in preparation). There is an excellent match between the black curve and the points, indicating that mergers are not required to explain the mass evolution of large spiral galaxies.

proximately constant at $10-15\,M_\odot$ yr^{-1} from $z \sim 2.5$ to $z \sim 1$ and then decreases rapidly to $\lesssim 2\,M_\odot$ yr^{-1} at $z = 0$. The form of this star formation history is well approximated by

$$\log(1 + \text{SFR}) = 0.26 + 0.92z - 0.23z^2. \qquad (2)$$

This evolution is qualitatively consistent with the color evolution seen in Fig. 2, as the galaxies become rapidly redder in rest-frame $u-g$ at $z < 1$. More to the point, Eq. 2 is consistent with the actual star formation rates of the galaxies: the points with errorbars in Fig. 4b show the mean star formation rates of the galaxies that went into the analysis, as obtained from SED fits (see Kriek et al. 2009, and Skelton et al., in preparation). This consistency implies that the assembly history can be fully explained by star formation and that mergers likely played a minor role. This can, again, be contrasted with more massive galaxies, as star formation is not sufficient to explain their growth after $z \sim 1.5$ (van Dokkum et al. 2010).

3.4. *Structural Evolution*

Finally, we quantify the implications of our results for the structural evolution of galaxies with the present-day mass of the Milky Way. As the mass growth is mostly independent of radius, we expect the structure of the galaxies to remain more or less the same over cosmic time. The evolution of the GALFIT-derived structural parameters of the stacks (see § 3.2) is shown in Fig. 5.

The effective radii and Sersic indices have indeed changed relatively little since $z \sim 2.5$, particularly when it is considered that the galaxies increased in mass by a factor of ~ 10 over this time. The radius increased by a factor ~ 1.8 and the Sersic index changed from $n \sim 1.5$ to $n \sim 2.5$. The red curves show the change in these same parameters for high mass galaxies, calculated in the same way (Patel et al. 2013a). Even though the progenitors of today's massive galaxies increased their mass by only a factor of ~ 3 over this redshift range they show much more dramatic structural evolution.

This point is emphasized in Fig. 5c,d which compares the structural evolution to the mass evolution for both classes of

galaxies. The sizes of massive galaxies grow as $r_e \propto M^2$ (van Dokkum et al. 2010; Hilz et al. 2013; Patel et al. 2013a), whereas those of galaxies with the mass of the Milky Way grow as $r_e \propto M^{0.3}$. This slope is similar to that of the size-mass relation of late type galaxies (e.g., Shen et al. 2003). We note that an increase in Sersic index does *not* imply growth of a classical bulge for either class of galaxy (see also Nelson et al. 2013).

4. DISCUSSION

In this *Letter* we have demonstrated that it is possible to obtain a description of the formation of galaxies with the mass of the Milky Way all the way from $z \sim 2.5$ to the present. We find that these galaxies built up $\sim 90\,\%$ of their stellar mass since $z \sim 2.5$. The build-up can be fully explained by the measured star formation rates of the galaxies, and does not require significant merging. The key result of our paper is that most of the mass growth took place in a uniform way, with the galaxies increasing their mass at approximately the same rate at all radii. Our results are therefore inconsistent with models in which bulges are fully assembled before disks: we do not find "naked bulges" at high redshift. Instead, they are consistent with models in which bulges (and presumably black holes) were largely built up at the same time as disks, through short-lived peaks in the accretion rate, bar instabilities, clump migration, or other processes (e.g., Debattista et al. 2006; Dekel et al. 2009). The implied star formation rate declines precipitously after $z \sim 1$, particularly in the central ≈ 2 kpc of the galaxies. By $z = 0$ we are left with quiescent bulges and slowly star forming disks.

Many other studies have reached similar conclusions using independent arguments; here we limit the discussion to a handful examples. Wuyts et al. (2011) and Nelson et al. (2013) find that star formation at high redshift typically occurs in disks. Nelson et al. (2012) find that galaxies begin to build inside-out at $z \sim 1$. As noted in § 1 Genzel et al. (2008), Förster Schreiber et al. (2011), and others have identified thick, clumpy star forming disks at $z \sim 2$. Finally, the in-
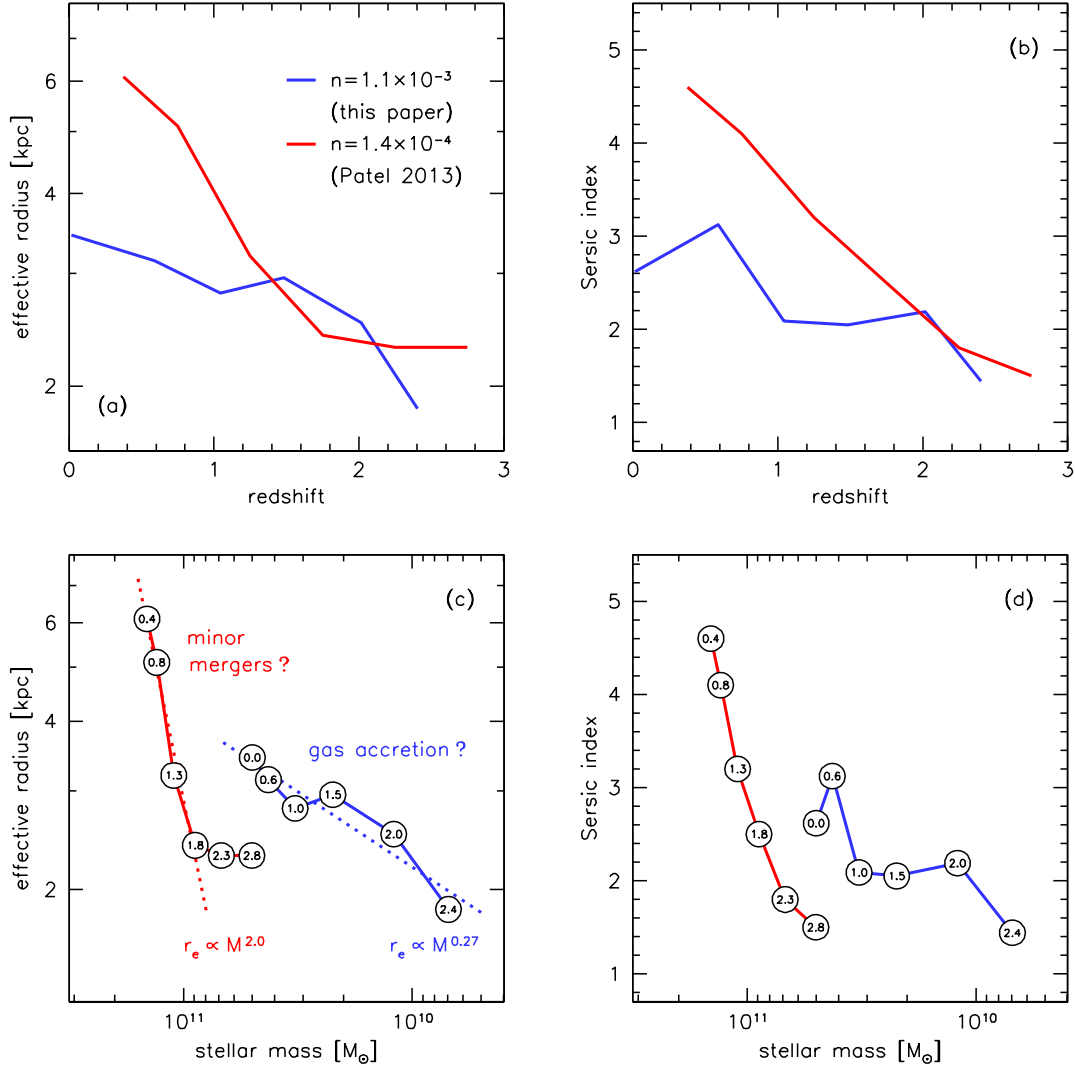
Figure 5. Effective radius and Sersic index as a function of redshift and mass, for Milky Way progenitors (blue) and more massive galaxies (red, taken from Patel et al. 2013a). Galaxies like the Milky Way have undergone much less structural evolution than the giant elliptical galaxies that populate the high mass end of the mass function.

ferred star formation history (Eq. 2) is consistent with the one derived by Behroozi, Wechsler, & Conroy (2012) for $10^{12} M_{\odot}$ halos, but is more peaked than the history inferred by Moster, Naab, & White (2013).

It is tempting to compare our results directly to known properties of the Milky Way itself; e.g., Eq. 2 implies a $z = 0$ star formation rate of $\sim 1\,M_{\odot}\,\mathrm{yr}^{-1}$, in reasonably good agreement with that of the Milky Way (Robitaille & Whitney 2010). We note, however, that the Milky Way has a relatively low bulge-to-disk ratio for its mass (e.g., McMillan 2011). Furthermore, the Milky Way, like any other galaxy, has had a unique history and it is fundamentally hazardous to apply the statistical analysis of samples of distant galaxy samples to an individual nearby galaxy (see, e.g., Fig. 1 of Leja et al. 2013).

As noted in previous Sections, the formation process of galaxies with $\log M \approx 10.7$ appears to be very different from that of more massive galaxies. Massive galaxies formed inside-out, with their extended wings assembling after formation of a compact core at high redshift. It will be interesting to see if galaxy formation models can reproduce both types of behavior seen in Fig. 5; e.g., it may be that (minor) merg-

ers lead to inside-out growth whereas gas accretion leads to uniform growth.

This study can be extended and improved in many ways. Most importantly, we have largely ignored systematic uncertainties in our analysis. Among the uncertainties are the low mass end of the mass function at $z > 2$ (see, e.g., Reddy & Steidel 2009); possible errors in the number density selection technique (Leja et al. 2013); systematic errors in redshifts and/or masses in the 3D-HST v2.1 catalogs; and the conversion of light-weighted to mass-weighted profiles. We have also ignored the spread in galaxy properties at fixed mass (see, e.g., Baldry et al. 2006; Franx et al. 2008, and Fig. 2). Finally, our analysis is, by its nature, indirect: we do not actually observe the formation of different parts of the galaxies but infer this from changes in their stellar surface densities. Stellar migration and other processes almost certainly altered the orbits of stars after their formation (Roškar et al. 2008). Deep, direct observations of spatially-resolved gas distributions at high redshift, particulary in the crucial epoch $1 < z < 2.5$, are needed to disentangle formation and migration, and to shed light on the physical processes that are at work (e.g., Nelson

et al. 2012, 2013; Freundlich et al. 2013).

REFERENCES

Agertz, O., Teyssier, R., & Moore, B. 2011, MNRAS, 410, 1391
Baldry, I. K., Balogh, M. L., Bower, R. G., Glazebrook, K., Nichol, R. C., Bamford, S. P., & Budavari, T. 2006, MNRAS, 373, 469
Behroozi, P. S., Wechsler, R. H., & Conroy, C. 2012, ArXiv e-prints
Brammer, G. B., van Dokkum, P. G., Franx, M., Fumagalli, M., Patel, S., Rix, H.-W., Skelton, R. E., Kriek, M., et al. 2012, ApJS, 200, 13
Brinchmann, J., Charlot, S., Heckman, T. M., Kauffmann, G., Tremonti, C., & White, S. D. M. 2004, ArXiv Astrophysics e-prints
Brooks, A. M., Solomon, A. R., Governato, F., McCleary, J., MacArthur, L. A., Brook, C. B. A., Jonsson, P., Quinn, T. R., et al. 2011, ApJ, 728, 51
Debattista, V. P., Mayer, L., Carollo, C. M., Moore, B., Wadsley, J., & Quinn, T. 2006, ApJ, 645, 209
Dekel, A., Birnboim, Y., Engel, G., Freundlich, J., Goerdt, T., Mumcuoglu, M., Neistein, E., Pichon, C., et al. 2009, Nature, 457, 451
Elmegreen, B. G., Bournaud, F., & Elmegreen, D. M. 2008, ApJ, 688, 67
Flynn, C., Holmberg, J., Portinari, L., Fuchs, B., & Jahreiß, H. 2006, MNRAS, 372, 1149
Förster Schreiber, N. M., Shapley, A. E., Erb, D. K., Genzel, R., Steidel, C. C., Bouché, N., Cresci, G., & Davies, R. 2011, ApJ, 731, 65
Franx, M., van Dokkum, P. G., Schreiber, N. M. F., Wuyts, S., Labbé, I., & Toft, S. 2008, ApJ, 688, 770
Freundlich, J., Combes, F., Tacconi, L. J., Cooper, M. C., Genzel, R., Neri, R., Bolatto, A., Bournaud, F., et al. 2013, ArXiv e-prints
Genzel, R., Burkert, A., Bouché, N., Cresci, G., Förster Schreiber, N. M., Shapley, A., Shapiro, K., Tacconi, L. J., et al. 2008, ApJ, 687, 59
Giavalisco, M., Ferguson, H. C., Koekemoer, A. M., Dickinson, M., Alexander, D. M., Bauer, F. E., Bergeron, J., Biagetti, C., et al. 2004, ApJ, 600, L93
Grogin, N. A., Kocevski, D. D., Faber, S. M., Ferguson, H. C., Koekemoer, A. M., Riess, A. G., Acquaviva, V., Alexander, D. M., et al. 2011, ApJS, 197, 35
Guedes, J., Callegari, S., Madau, P., & Mayer, L. 2011, ApJ, 742, 76
Hilz, M., Naab, T., & Ostriker, J. P. 2013, MNRAS, 429, 2924
Ilbert, O., McCracken, H. J., Le Fevre, O., Capak, P., Dunlop, J., Arnouts, S., Aussel, H., Caputi, K., et al. 2013, ArXiv e-prints
Kauffmann, G., White, S. D. M., & Guiderdoni, B. 1993, MNRAS, 264, 201
Kitzbichler, M. G. & White, S. D. M. 2008, MNRAS, 391, 1489
Koekemoer, A. M., Faber, S. M., Ferguson, H. C., Grogin, N. A., Kocevski, D. D., Koo, D. C., Lai, K., Lotz, J. M., et al. 2011, ApJS, 197, 36
Kriek, M., van Dokkum, P. G., Labbé, I., Franx, M., Illingworth, G. D., Marchesini, D., & Quadri, R. F. 2009, ApJ, 700, 221
Kroupa, P. 2001, MNRAS, 322, 231
Krumholz, M. R. & Dekel, A. 2010, MNRAS, 406, 112

Leja, J., van Dokkum, P., & Franx, M. 2013, ApJ, 766, 33
Marchesini, D., van Dokkum, P. G., Förster Schreiber, N. M., Franx, M., Labbé, I., & Wuyts, S. 2009, ApJ, 701, 1765
McMillan, P. J. 2011, MNRAS, 414, 2446
Mo, H. J., Mao, S., & White, S. D. M. 1998, MNRAS, 295, 319
Moster, B. P., Naab, T., & White, S. D. M. 2013, MNRAS, 428, 3121
Moustakas, J., Coil, A., Aird, J., Blanton, M. R., Cool, R. J., Eisenstein, D. J., Mendez, A. J., Wong, K. C., et al. 2013, ArXiv e-prints
Muzzin, A., Marchesini, D., Stefanon, M., Franx, M., McCracken, H. J., Milvang-Jensen, B., Dunlop, J. S., Fynbo, J. P. U., et al. 2013, ArXiv e-prints
Nelson, E. J., van Dokkum, P. G., Brammer, G., Förster Schreiber, N., Franx, M., Fumagalli, M., Patel, S., Rix, H.-W., et al. 2012, ApJ, 747, L28
Nelson, E. J., van Dokkum, P. G., Momcheva, I., Brammer, G., Lundgren, B., Skelton, R. E., Whitaker, K. E., Da Cunha, E., et al. 2013, ApJ, 763, L16
Okamoto, T. 2013, MNRAS, 428, 718
Papovich, C., Finkelstein, S. L., Ferguson, H. C., Lotz, J. M., & Giavalisco, M. 2011, MNRAS, 412, 1123
Patel, S. G., van Dokkum, P. G., Franx, M., Quadri, R. F., Muzzin, A., Marchesini, D., Williams, R. J., Holden, B. P., et al. 2013a, ApJ, 766, 15
Patel, S. G., et al. 2013b, ApJL, submitted
Peng, C. Y., Ho, L. C., Impey, C. D., & Rix, H.-W. 2010, AJ, 139, 2097
Reddy, N. A. & Steidel, C. C. 2009, ApJ, 692, 778
Rix, H.-W. & Bovy, J. 2013, ArXiv e-prints
Robitaille, T. P. & Whitney, B. A. 2010, ApJ, 710, L11
Roškar, R., Debattista, V. P., Quinn, T. R., Stinson, G. S., & Wadsley, J. 2008, ApJ, 684, L79
Sales, L. V., Navarro, J. F., Theuns, T., Schaye, J., White, S. D. M., Frenk, C. S., Crain, R. A., & Dalla Vecchia, C. 2012, MNRAS, 423, 1544
Sersic, J. L. 1968, Atlas de galaxias australes (Cordoba, Argentina: Observatorio Astronomico, 1968)
Shen, S., Mo, H. J., White, S. D. M., Blanton, M. R., Kauffmann, G., Voges, W., Brinkmann, J., & Csabai, I. 2003, MNRAS, 343, 978
Szomoru, D., Franx, M., van Dokkum, P. G., Trenti, M., Illingworth, G. D., Labbé, I., Bouwens, R. J., Oesch, P. A., et al. 2010, ApJ, 714, L244
Szomoru, D., Franx, M., van Dokkum, P. G., Trenti, M., Illingworth, G. D., Labbé, I., & Oesch, P. 2013, ApJ, 763, 73
van Dokkum, P. G., Whitaker, K. E., Brammer, G., Franx, M., Kriek, M., Labbé, I., Marchesini, D., Quadri, R., et al. 2010, ApJ, 709, 1018
Wuyts, S., Forster Schreiber, N. M., van der Wel, A., Magnelli, B., Guo, Y., Genzel, R., Lutz, D., Aussel, H., et al. 2011, ArXiv e-prints
Zoccali, M., Lecureur, A., Barbuy, B., Hill, V., Renzini, A., Minniti, D., Momany, Y., Gómez, A., et al. 2006, A&A, 457, L1